



# Seasonal patterns and multidecadal trends in phytoplankton functional groups in the Benguela upwelling system off Namibia

Tebatso M. Moloto<sup>a,b,\*</sup>, Marié E. Smith<sup>d,e</sup>, Thomas G. Bell<sup>f</sup>, Stuart J. Piketh<sup>b</sup>, Sandy J. Thomalla<sup>a,c</sup>

<sup>a</sup> Southern Ocean Carbon-Climate Observatory (SOCCO), Council for Scientific and Industrial Research (CSIR), Rosebank, Cape Town, South Africa

<sup>b</sup> Unit for Environmental Sciences and Management, North-West University, Potchefstroom, South Africa

<sup>c</sup> Marine and Antarctic Research Centre for Innovation and Sustainability (MARIS), University of Cape Town, Rondebosch, South Africa

<sup>d</sup> Coastal Systems and Earth Observation Research Group, CSIR, Cape Town, South Africa

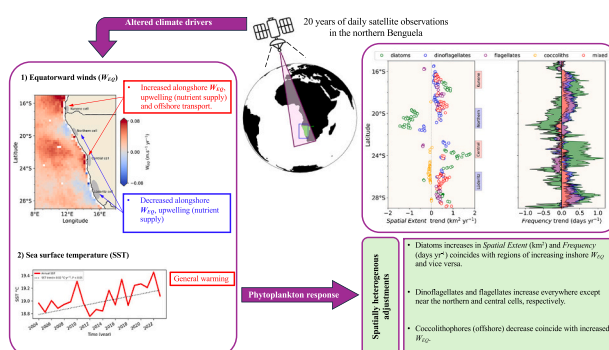
<sup>e</sup> Department of Oceanography, University of Cape Town, Cape Town, South Africa

<sup>f</sup> Plymouth Marine Laboratories, Prospect Place, The Hoe, PL1 3DH Plymouth, United Kingdom

## HIGHLIGHTS

- Distribution patterns of PFGs exhibit evidence of regional preference for dominance.
- There's evidence of niche SST and equatorward wind occupation for each PFG.
- PFGs expand at distinct seasonal timings, except for declining coccolithophores.
- Diatoms have a stronger sensitivity in their response to environmental changes.
- Altered coastal equatorward winds are a key driver of diatom adjustments.

## GRAPHICAL ABSTRACT



## ARTICLE INFO

### Keywords:

Satellite  
Remote sensing  
Phytoplankton  
Benguela upwelling system  
Climate change  
MODIS-aqua  
Namibia

## ABSTRACT

Understanding the response of phytoplankton to climate change is crucial for predicting shifts in marine ecosystems. Despite the Benguela being the world's most productive eastern boundary upwelling system, the distribution and susceptibility of its phytoplankton functional groups (PFGs) to climate change remain poorly understood. Here, we use 20 years (2003–2022) of daily MODIS-Aqua satellite data to uncover distinct spatial, seasonal and multidecadal trends in key PFGs (diatoms, dinoflagellates, flagellates, coccolithophores). PFGs exhibit strong regional and seasonal variability in their *Spatial Extent* and *Frequency* of dominance, with evidence of niche conditions favoring particular PFGs. Multidecadal trends reveal strong spatial variability in PFG adjustments, which are closely aligned with major upwelling cells. Some cells show increasing diatom dominance coupled with declines in coccolithophores, dinoflagellates and flagellates, while others exhibit the opposite trend. Seasonal transitions are also evident, with diatom-to-dinoflagellates shifts in Summer and enhanced diatom dominance in Autumn. Overall, PFGs increased in *Spatial Extent* and *Frequency* of dominance at distinct

\* Corresponding author at: Southern Ocean Carbon-Climate Observatory (SOCCO), Council for Scientific and Industrial Research (CSIR), Rosebank, Cape Town, South Africa.

E-mail address: [tebatso.martin@gmail.com](mailto:tebatso.martin@gmail.com) (T.M. Moloto).

<https://doi.org/10.1016/j.scitotenv.2025.180217>

Received 15 October 2024; Received in revised form 4 August 2025; Accepted 4 August 2025

0048-9697/© 2025 The Authors. Published by Elsevier B.V. This is an open access article under the CC BY license (<http://creativecommons.org/licenses/by/4.0/>).

seasonal timings, except for declining coccolithophores. The link between alongshore equatorward winds and PFG trends strongly suggests an altered nutrient supply-driven response. Diatoms, significant carbon exporters, exhibit pronounced adjustments, highlighting their sensitivity to environmental changes. These findings are indicative of potential impacts on biogeochemical cycling and higher trophic levels, affecting carbon export and marine services. These insights provide a critical foundation for identifying climate-sensitive regions and seasonal windows of ecological vulnerability, supporting the development of early warning systems for adaptive conservation efforts.

## 1. Introduction

Marine phytoplankton form the base of the aquatic food-web sustaining higher trophic levels and lucrative fisheries. In addition, phytoplankton production and export modulate biogeochemical cycling with important impacts on climate regulation (Charlson et al., 1987; Field et al., 1998). These photosynthetic microorganisms are conceptually grouped into phytoplankton functional groups (PFGs) according to common ecological traits (Reynolds et al., 2002). Diatoms are considered effective exporters of carbon to the deep ocean and to higher trophic levels (Allen et al., 2005) while smaller dinoflagellates and calcifying coccolithophores are important producers of the climatically active dimethyl sulfide (DMS) gas, which seeds aerosol and cloud formation and impacts climate (Charlson et al., 1987). Collectively, phytoplankton occupy key roles in ecosystem functioning, food security and climate, which makes them ideal indicators of overall ecosystem health and trophic status (Tweddle et al., 2018). Phytoplankton community composition and succession are intricately tied to a complex interplay of physical and biogeochemical factors that dictate the characteristics of their environment (e.g. temperature, water column stability, light and nutrient availability) (Araújo et al., 2022). Continued anthropogenic carbon emissions are altering many of these

environmental forcing mechanisms that promote or constrain phytoplankton growth (Calvin et al., 2023), with evidence of change already apparent in bloom phenology (Thomalla et al., 2023), frequency and spatial occupation (Dai et al., 2023) and abundance (Van Oostende et al., 2023), with far reaching implications for marine ecosystem services. Understanding long-term spatiotemporal trends in phytoplankton dynamics, particularly in highly productive ocean regions, is fundamental to our ability to detect early ecosystem disturbances and predict the magnitude and direction of ecosystem shifts. Such knowledge is vital for informed decision-making and the implementation of effective conservation and management strategies for sustainable ecosystems and the preservation of the key services that they elicit.

Eastern Boundary Upwelling Systems (EBUS) are coastal oceanic regions characterized by equatorward wind-driven upwelling of cold nutrient-enriched subsurface waters to the euphotic zone where they fuel high rates of primary production that manifest as phytoplankton blooms (Kämpf and Chapman, 2016). Although comprising <7 % of the global ocean, EBUS offer great socio-economic services by accounting for ~2 % of global ocean production and ~20 % of global fisheries yields (Carr and Kearns, 2003). The Benguela upwelling system (BUS) off South West Africa (Fig. 1) is divided into its northern (nBUS) and southern (sBUS) components and is considered the most productive of

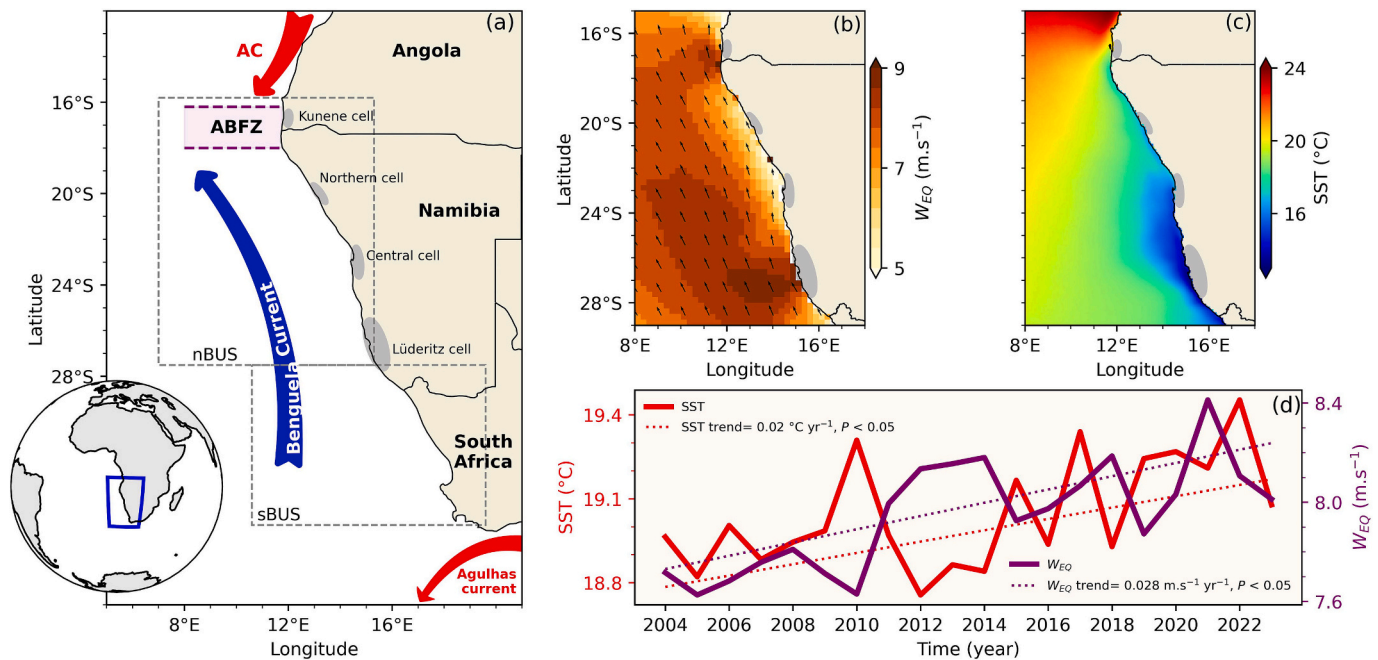


**Fig. 1.** Study area, mean phytoplankton abundance as well as long term dynamics of key climate drivers.

**a,** The Benguela upwelling system along the south western tip of the African continent (inset) shared between South Africa, Namibia and Angola (shown in bold) with its northern (nBUS) and southern (sBUS) subsystems indicated by dashed gray boxes. Upwelling centers in the nBUS are indicated as gray shaded areas, the Angola-Benguela frontal zone (ABFZ) is indicated by the purple shaded area. The cold Benguela current is shown by the blue arrow whereas the warm Agulhas and Angola (AC) currents are shown by the red arrows. **b,** Mean equatorward winds speed ( $W_{EQ}$ ) at 10 m above sea surface with wind direction (black arrows) overlaid, computed from the zonal (U) and meridional (V) wind components (European Union-Copernicus Marine Service, 2017). **c,** Sea surface temperature (SST) climatology (MODIS-Aqua, Level-3 4 km), with gray shaded areas in **b** and **c** also representing upwelling cells. **d,** Long-term trends in key climate drivers, SST and  $W_{EQ}$ , showing the imprint of climate change manifested as warming and wind acceleration. The red and purple solid lines represent mean annual SSTs and  $W_{EQ}$ , respectively, with dotted lines indicating long-term annual trends. Trends are considered statistically significant when  $P < 0.05$ . Climatological means of Chl-a,  $W_{EQ}$  and SST (**a**, **b**, **c**) as well as annual means for trends analysis (**d**) were computed from daily satellite observations between 01 January 2003–31 December 2022.

the four main EBUS (Carr, 2001). The nBUS off Namibia and Angola is progressively being impacted by climate change via increasing sea surface temperatures (Fig. 1d), intensifying equatorward winds (Fig. 1d), expanding oxygen-minimum zones (Monteiro et al., 2008) and altered wind-driven upwelling (Lamont et al., 2018) in addition to human-induced activities such as overfishing (Cury and Shannon, 2004). Plankton communities at the base of this key marine ecosystem are likely to be impacted by these altered climate dynamics with consequential changes expected in their composition and distribution patterns with cascading ramifications for ecosystem function. For example, increasing SST coupled with decreasing dissolved oxygen concentrations have been reported to constrain vertical plankton distributions and the survival of early life-cycle stages of fish (Auel and Verheye, 2007; Ekau and Verheye, 2005).

Continuous environmental monitoring programmes provide long-term datasets that are essential to ecosystem assessment for effective environmental management efforts (Benway et al., 2019). Shipboard observations are severely constrained both spatially (distinct geographic transects) and temporally (monthly to seasonal occupations), making an ecosystem-wide response of phytoplankton communities to climate variability difficult to detect. Satellite remote sensing has advanced our ability to observe and monitor surface ocean dynamics at high temporal (daily, spanning years to decades) and spatial (300 m, global coverage) scales. While spatial and temporal trends in chlorophyll *a* (Chl-*a*) concentration (Demarcq, 2009), Chl-*a* size fractions (Lamont et al., 2019) and bloom occurrence (Dai et al., 2023) have been examined in the BUS, much less is known about the dynamics of specific phytoplankton functional groups (PFGs) over climate-relevant time scales. In particular, the response of PFGs to climate-driven changes such as warming and shifting wind patterns, remains poorly constrained in the Benguela upwelling system, the world's most productive EBUS. This gap is critical, as PFGs play distinct roles in biogeochemical cycling, food web dynamics, and carbon export. Moreover, the lack of long-term, spatially explicit assessments of PFG climatology and variability hampers our ability to predict how marine ecosystems may respond to ongoing climate change. To address this gap, we utilize 20 years of daily MODIS-Aqua satellite data to characterize the seasonal patterns of key PFGs (diatoms, dinoflagellates, flagellates, and coccolithophores) and assess their long-term trends in the context of the physical climate drivers of SST and equatorward wind patterns in the nBUS. The hypothesis being that shifts in environmental drivers will lead to changes in the relative abundance of PFGs, with certain groups gaining dominance as they become better suited to the emerging conditions. By doing so, this study provides new insights into the spatial and seasonal dynamics of key PFGs and their links to physical drivers, with implications for ecosystem functioning and climate resilience.

## 2. Methods

### 2.1. Study region

The BUS is situated on the southwestern coast of the African continent, stretching from Cape Agulhas in South Africa along the Namibian coast and northwards into Angola (Fig. 1a). The BUS is unique to other EBUS in that it is bound by two warm water masses, the Agulhas current in the south and the Angola current in the north (Fig. 1a) (Kämpf and Chapman, 2016). Of the four EBUS, the BUS is estimated to be the most productive (Carr, 2001). The study was conducted in the northern Benguela Upwelling System (nBUS), situated off the coast of Namibia (Fig. 1a). The nBUS is influenced by two different water masses: The dominant surface currents are the poleward flowing warm Angola Current (AC) and its northward flowing cold Benguela Current (BC) counterpart, which converge at the Angola Benguela Frontal Zone (ABFZ) with a seasonally and interannually variable geolocation between 15 and 18°S that separates the oligotrophic tropical ecosystem to the north from the nutrient-rich BUS to the south (Fig. 1a) (Kämpf and

Chapman, 2016).

The nBUS is characterized by strong and seasonally variable equatorward alongshore wind jets that induce coastal upwelling of the deep, cold and nutrient-rich waters to the sunlit ocean surface (Kämpf and Chapman, 2016). Once upwelled, the nutrient-enriched surface waters fuel marine primary production, which manifests in the form of phytoplankton blooms (Louw et al., 2016). There are four upwelling cells in the nBUS, viz. The Kunene, Northern, Central and lastly the largest, most intense, and perennial Lüderitz upwelling cell located at ~26°S that partitions the BUS into its northern (nBUS) and southern (sBUS) sub-systems (Fig. 1a).

### 2.2. Ocean color satellite remote sensing data

Daily level-3 (L3) ocean color remote sensing data with 4 km spatial resolution from the Moderate Resolution Imaging Spectroradiometer aboard NASA's aqua satellite (MODIS-Aqua) were obtained from the NASA Ocean Color web (<https://oceancolor.gsfc.nasa.gov/>). Ocean color data were obtained for the normalized fluorescence line height (nFLH,  $\text{mW m}^{-2} \mu\text{m}^{-1} \text{sr}^{-1}$ ), remote sensing reflectance ( $R_{rs}$ ,  $\lambda$ ;  $\text{sr}^{-1}$ ) at 443 ( $R_{rs443}$ ), 488 ( $R_{rs488}$ ), 531 ( $R_{rs531}$ ), 547 ( $R_{rs547}$ ), 667 ( $R_{rs667}$ ) and 678 ( $R_{rs678}$ ) nm wavebands as well as sea surface temperature (SST, °C) and chlorophyll-*a* (Chl-*a*,  $\mu\text{g.l}^{-1}$ ). The daily ocean color remote sensing data spanned the period from January 2003 to December 2022, with a total of 65,619 daily satellite data files.

### 2.3. PFG remote sensing detection proxies

The regional algorithm derived for MODIS-Aqua application of Moloto et al. (2023) was applied for the detection of phytoplankton functional group dominance (diatoms, flagellates, and low and high biomass dinoflagellates) in the northern Benguela upwelling system. Dominance, according to the algorithm, is acquired when a PFG contributes more than 50 % to the total phytoplankton community biomass at any given time and location. In cases where no single PFG contributes more than 50 % to the total community, the algorithm classifies the assemblage as a mixed community. The strength of this approach lies in its ability to represent ecologically plausible scenarios of co-dominance; however, a limitation is that it does not specify which groups comprise the mixed assemblage. The authors used statistical thresholds based on dual band ratios of spectral bands in the green, red and near-infrared regions (531, 547, 667 and 748 nm) as well as spectral band difference (nFLH) proxies to exploit small variations in  $R_{rs}$  characteristics of waters associated with dominance of PFGs. In the current study, we combine the low and high biomass dinoflagellates and report them as one dinoflagellate PFG.

Coccolithophore blooms were detected using an adaptation of the approach of Smith et al. (2023), which utilizes the distinctive blue-green reflectance peak caused by coccolithophore blooms. The original detection technique operates on the Sea-viewing Wide Field-of-view Sensor (SeaWiFS) data and calculates the integral of  $R_{rs}$  between 490 and 510 nm. SeaWiFS however has a limited temporal coverage (September 1997 to December 2010), thus limiting its suitability for this study. Accordingly, we adopted the algorithm for application to MODIS-Aqua observations. In the absence of MODIS-Aqua  $R_{rs490}$  and  $R_{rs510}$  wavebands, our adaptation instead calculates the integral of  $R_{rs}$  between 488 and 531 nm. An integral threshold of 0.26 was used since it corresponds to a minimum threshold of approximately  $2 \text{ mmol m}^{-3}$  of particulate inorganic carbon (PIC) in the MODIS-Aqua PIC product in confirmed offshore bloom areas (data not shown). A PIC of  $2 \text{ mmol m}^{-3}$  is often used as a threshold for detecting coccolithophore blooms (He et al., 2022). Additional classification criteria included excluding pixels from potentially suspended sediment-laden waters with a peak in the green spectral band ( $R_{rs488} > R_{rs547}$ ) and the exclusion of pixels potentially affected by anomalously elevated reflectance in the blue spectral band ( $R_{rs488} > R_{rs443}$ ). Near-shore coccolithophore-like

features in Namibia have been demonstrated to be a result of hydrogen sulfur ( $\text{H}_2\text{S}$ ) eruptions in the shelf ( $< 200$  m depth) (Ohde et al., 2007), which have similar spectral features to coccolithophores (Siegel et al., 2007). In order to avoid misclassification of these events as coccolithophore blooms, we masked out the pixels where the bathymetry (GEBCO Bathymetric Compilation Group 2023, 2023) was less than 200 m.

#### 2.4. PFG quantitative indices

Two quantitative indices were derived following application of the PFG algorithms to allow for a spatiotemporal analysis of the 7291 daily satellite observations in the nBUS. These included 1) *Frequency* – calculated as the number of days of dominance per pixel by each PFG on an annual or seasonal time scale (days per year/season), and 2) *Spatial Extent* – defined as the area dominated by each PFG, calculated as the sum of all 4-km pixels dominated by each PFGs and converted to area ( $\text{km}^2$ ) by accounting for the spatial resolution of the MODIS-Aqua pixels.

#### 2.5. Equatorward winds

The Global Ocean Daily Gridded Reprocessed level-3 (L3) Sea Surface Winds from Scatterometer (European Union-Copernicus Marine Service, 2017) was selected as the best (of four) wind data product for the region from a comparison with QuickSCAT (see Supplementary Material for detailed comparative study). The meridional (V) and zonal (U) wind vector components at 10 m above sea surface were used to compute equatorward winds ( $W_{EQ}$ ).

#### 2.6. Trends analysis

Annual and seasonal *Frequency*, *Spatial Extent*, SST and  $W_{EQ}$  time series datasets were computed from daily satellite observations and constitute the main material to compute linear trends analysis. Prior to trends analysis, we applied quality control measures to mitigate the influence of missing data and outliers (anomalous data) to minimize error and bias following the approach of Thomalla et al. (2023). Firstly, pixels with less than 50 % of the total time series (i.e.  $< 10$  years) of valid observations were excluded from statistical trend analysis to ensure temporal robustness and minimize bias from data gaps. Secondly, the datasets were tested for normality of their distribution. If the data were normally distributed, then linear regressions were performed using the robust Huber-Regression (epsilon ( $\epsilon$ ) = 1.35). The Huber regression analysis is considered to be robust as it is less sensitive to outliers and limits their impact on trends estimates. If the data were not normally distributed, then linear regression analysis was performed using the non-parametric Mann-Kendall (MK) test.

#### 2.7. Correlation of trends on PFGs with SST and equatorward winds

To assess the correlation between long-term changes in key climate drivers of SST and  $W_{EQ}$  with PFGs, we first regridded  $W_{EQ}$  onto the 4 km MODIS-Aqua grid using the nested2gd method of the xESMF python package (version v0.8.2). Then we linearly correlated the PFG indices (i.e. *Spatial Extent*, *Frequency*) against SST and  $W_{EQ}$  and quantified the strength of their association using Pearson's correlation coefficient ( $r$ ).

### 3. Results

#### 3.1. Climatological patterns and environmental drivers of PFGs

The occurrence and distribution of PFGs in the nBUS is primarily mediated by nutrient supply, temperature, light and turbulence (Hansen et al., 2014). Equatorward winds ( $W_{EQ}$ ) drive coastal upwelling, which impacts temperature, turbulence, water column structure, nutrient and light supply (Mohrholz et al., 2014). As such, these winds play a key role

in determining the physicochemical environment that supports phytoplankton production, with different PFGs outcompeting others in the spectrum of conditions that vary both regionally (i.e. inshore/offshore, north/south) and temporally (i.e. on event/seasonal/annual and multi-decadal time scales) (Hansen et al., 2014; Louw et al., 2016; Siegel et al., 2007).

In this study, we use *Frequency* ( $\text{days yr}^{-1}$ ) and *Spatial Extent* ( $\text{km}^2$ ) as metrics to study spatiotemporal variability in PFG dominance. Climatological maps from the past 20 years of annual mean *Frequency* (Fig. 2A) reveal that diatoms dominate most frequently ( $\leq 80$  days  $\text{yr}^{-1}$ ), followed by flagellates and mixed communities ( $\leq 30$  days  $\text{yr}^{-1}$ ) with moderate frequency of dominance by dinoflagellates ( $\leq 16$  days  $\text{yr}^{-1}$ ) and infrequent coccolithophore dominance ( $< 2$  days  $\text{yr}^{-1}$ ). A poleward gradient of increasing *Frequency* is observed for all PFGs, with the highest frequencies occurring South of  $20^\circ\text{S}$  (Fig. 2A), consistent with a poleward decrease in SST (Fig. 1c), that is typically aligned with increased nutrient supply to the euphotic zone from  $W_{EQ}$ -driven upwelling (Fig. 1B). Diatoms show a classical inshore-offshore gradient (Fig. 2A) that is consistent with Chl-*a* (Fig. S1 of the Supplementary Material), with the highest *Frequencies* observed in high Chl-*a* coastal waters. Diatoms are highly competitive in cold, nutrient-rich environments following upwelling and are regular blooming PFGs that, together with dinoflagellates, contribute the largest proportion to phytoplankton Chl-*a* biomass in the nBUS (Fig. S1 of the Supplementary Material). In contrast, flagellates, dinoflagellates, coccolithophores and mixed phytoplankton communities tend to dominate in offshore waters coincident with moderate to low Chl-*a* concentrations (Fig. 2A, Fig. S1 of the Supplementary Material).

Examining PFGs *Frequency* in the context of SST and  $W_{EQ}$  (Fig. 2B, Fig. S2 of the Supplementary Material) reveals evidence of niche conditions favoring different PFGs. Diatoms are more frequently associated with cold conditions and rarely dominate in temperatures greater than  $17^\circ\text{C}$ . Although they occupy a broad range of  $W_{EQ}$ , their maximum frequencies are associated with less windy ( $< 7$   $\text{m.s}^{-1}$ ) conditions. In contrast, dinoflagellates most frequently dominate in warmer ( $16\text{--}19^\circ\text{C}$ ) conditions, although a few instances of high *Frequency* were also evident in cold ( $< 14^\circ\text{C}$ ) and windy ( $> 8$   $\text{m.s}^{-1}$ ) conditions. Flagellates and mixed communities occupy a broad SST and  $W_{EQ}$  range but prevail in conditions that are relatively cooler than dinoflagellates ( $< 17^\circ\text{C}$ ) and windier than diatoms ( $> 7$   $\text{m.s}^{-1}$ ). The few occasions of coccolithophore dominance tend to coincide with moderate temperature ( $16\text{--}19^\circ\text{C}$ ) and wind ( $> 6.5$   $\text{m.s}^{-1}$ ) conditions (Fig. 2B, Fig. S2 of the Supplementary Material).

All PFGs characteristically increase in *Spatial Extent* with increasing latitude from  $15^\circ\text{S}$  to  $\sim 25^\circ\text{S}$ , consistent with decreasing SST and increasing  $W_{EQ}$  (Fig. 3A). This is followed by a sharp decline at approximately  $25\text{--}28^\circ\text{S}$  that coincides with maximum  $W_{EQ}$  speeds ( $> 8.5$   $\text{m.s}^{-1}$ ) near the Lüderitz upwelling cell (Fig. 3A, Fig. 1B). This decline in PFG *Spatial Extent* results from the cumulative effect of enhanced turbulence and dynamic circulation that acts as a biological boundary constraining phytoplankton growth and biomass accumulation (Agenbag and Shannon, 1988). An assessment of the seasonal cycle in *Spatial Extent* in the context of SST and  $W_{EQ}$  climatologies reveals differences in the magnitude and timing of PFG peaks (Fig. 3B, red stars) that reflects a seasonal succession of community dominance. Dinoflagellates are the first to peak in April (early-autumn) during high  $W_{EQ}$  speeds (Fig. 3B, blue line), followed by diatoms in May (late-Autumn) coinciding with a relaxation of  $W_{EQ}$  and declining temperatures. Flagellates peak in June (early-winter), while mixed communities in July (mid-winter) and finally coccolithophores in November (late-Spring). Except for coccolithophores, all PFGs exhibit a seasonal minimum between September and March (warmer periods) coinciding with peak summer SSTs and minimum  $W_{EQ}$  (Fig. 3B). Coccolithophores flourish in warmer summer waters (Fig. 3B). Despite differences in the seasonal timing of *Spatial Extent* peaks, diatoms remain spatially dominant throughout the annual cycle and are not succeeded by any other



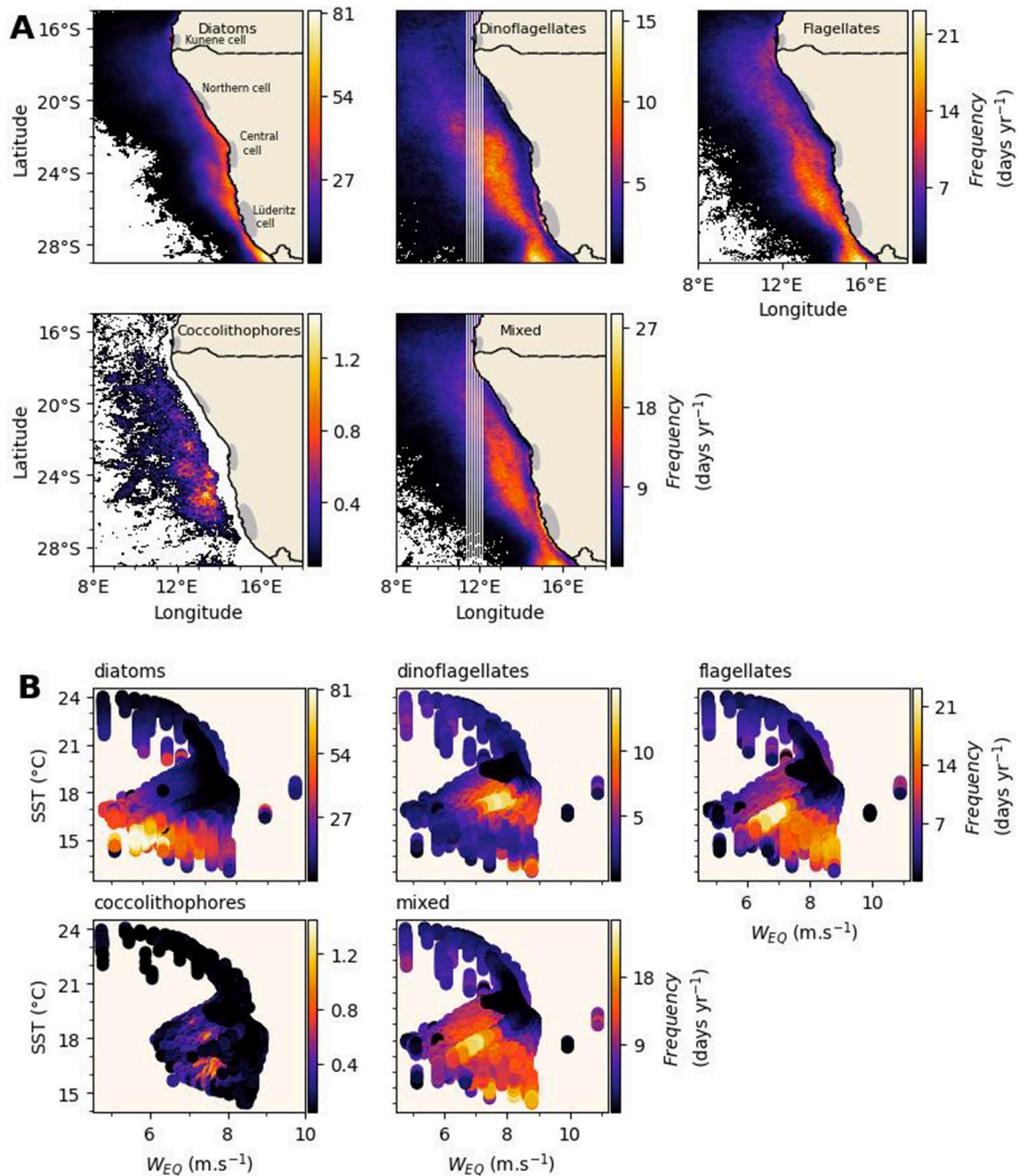


**Fig. 2.** Spatial climatological patterns of phytoplankton groups in the nBUS between 2003 and 2022.

**a,** Spatial climatological annual mean Frequency of dominance by PFGs from daily MODIS-Aqua satellite observations. Only observations at depths >200 m are shown for coccolithophores to the exclusion of coastal hydrogen sulfide ( $H_2S$ ) eruption plumes which have the same spectral features as offshore coccolithophore blooms (Siegel et al., 2007). **b,** Scatter plot of spatial climatological mean sea surface temperatures (SST, °C) and equatorward winds speed ( $W_{EQ}$ , m.s<sup>-1</sup>) with annual mean Frequency overlaid (color bar) to highlight mean PFG niche occupations of SST and  $W_{EQ}$  on 20-year climatological time scales.

PFG (Fig. S3 of the Supplementary Material). Seasonal succession in *Spatial Extent* is however observed in March and April when flagellate spatial dominance overtakes dinoflagellates and mixed populations respectively, with dinoflagellates recovering *Spatial Extent* dominance over flagellates in July (Fig. S3 of the Supplementary Material).

These results provide a more comprehensive and previously unobserved synoptic-scale account of regional and seasonal variability of key PFGs in the nBUS at unprecedented spatiotemporal scales. The observed regional and seasonal patterns reveal niche SST and  $W_{EQ}$  affinities that are favorable to the dominance of distinct PFGs in both time (seasonal succession) and space (north/south – inshore/offshore gradients).

Mapping the spatio-temporal variability of key PFGs provides critical insights into ecosystem dynamics.

### 3.2. Evidence of warming and altered equatorward winds

The nBUS is impacted by general warming of  $0.02\text{ }^{\circ}\text{C yr}^{-1}$  (Fig. 1D), with the most northerly region (near the Kunene cell) warming at a faster rate of up to  $0.1\text{ }^{\circ}\text{C yr}^{-1}$  (Fig. 4A), amounting to maximum temperature changes of as much as  $2\text{ }^{\circ}\text{C}$  over the 20-year time period. This general warming trend is consistent across all seasons, however small patches of coastal cooling ( $-0.1\text{ }^{\circ}\text{C yr}^{-1}$ ) are observed off the Kunene

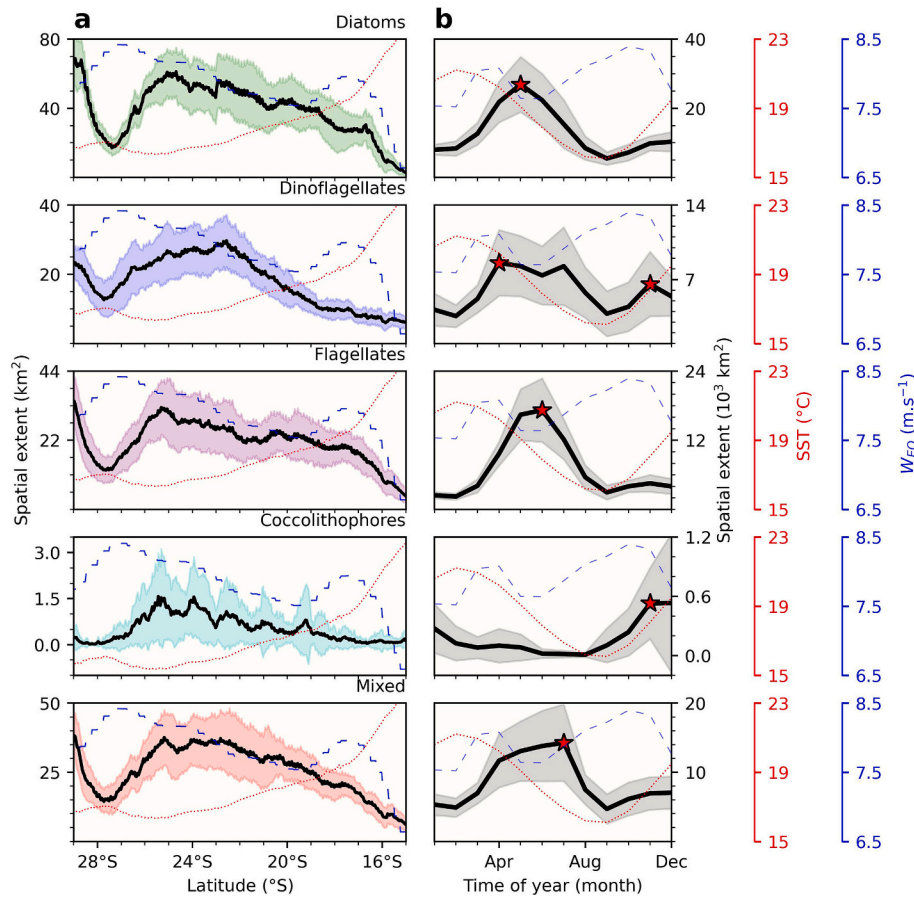


**Fig. 3.** PFGs Spatial Extent climatology in the past two decades (2003–2022).

**a**, Annual mean cross-shelf latitudinal distribution in *Spatial Extent* (solid black line) of PFG dominance. The shaded areas represent the degree of interannual variability in *Spatial Extent* calculated as the standard deviation. **b**, Corresponding annual cycle of *Spatial Extent* in PFG dominance (solid black line) showing the typical PFG seasonal succession in the timing of peak *Spatial Extent* (red stars) and degree of variability (gray shaded areas, determined as standard deviation). The red (dotted) and blue (dashed) lines in panels **a** and **b** represent annual mean sea surface temperatures (SST) and equatorward winds speed ( $W_{EQ}$ ) respectively. All annual mean values were computed from daily satellite observations between January 2003 – December 2022. Note the varying scales of the *Spatial Extent* in panels **a** and **b** as well as among PFGs.

cell in Summer and the Lüderitz cell in spring (Fig. S4 of the Supplementary Material). Trends in  $W_{EQ}$  are overwhelmingly positive (Fig. 1D,  $0.028 \text{ m s}^{-1} \text{ yr}^{-1}$ ), with coherent offshore increasing trends contrasting with the notable heterogeneity in alongshore trend patterns (Fig. 4B). Strong positive  $W_{EQ}$  trends are observed inshore off Kunene and Central cells ( $< 0.1 \text{ m s}^{-1} \text{ yr}^{-1}$ ) while smaller regions of negative trends are constrained to the coastlines of the Northern and Lüderitz cells ( $< -0.5 \text{ m.s}^{-1} \text{ yr}^{-1}$ ) (Fig. 4B). This spatial distribution in  $W_{EQ}$  trends is relatively consistent across all seasons but exacerbated in certain regions and seasons. For example, positive trends in  $W_{EQ}$  are dominant in Spring and Summer off the Kunene cell but in Autumn off the Central cell while the negative trends are largely absent in all seasons except Autumn (Fig. S4 of the Supplementary Material).

### 3.3. Multidecadal trends in PFGs

With the application of PFT algorithms to satellite ocean color data, we are now able to investigate the synoptic scale response of specific PFGs to adjustments in key environmental variables over two decades. A trends analysis of the annual *Frequency* ( $F_{trend}$ ) and *Spatial Extent* ( $SE_{trend}$ ) of PFGs reveals a heterogeneous distribution of significant ( $P < 0.05$ ) positive and negative trends, with evidence of regional cohesiveness in trend direction (Fig. 5 and Fig. 6). While  $F_{trend}$  reflects an increase or decrease in the frequency of dominance of PFGs (Fig. 5A), the  $SE_{trend}$  is indicative of a tendency to either expand (Fig. 6A, red circles) or shrink

(Fig. 6A, blue circles) in spatial occupation. Over the region as a whole, there are equal areas affected by positive and negative trends in diatoms  $F_{trend}$  (Fig. 5C). These trends are relatively consistent across inshore/offshore gradients (Fig. 5A) but alternate with latitude between positive and negative trends (Fig. 5B), with the Kunene and Central upwelling cells associated with increasing  $F_{trend}$  of diatom dominance, while the Northern and Lüderitz cells are instead associated with a decline. Notably, the increasing trends off the Kunene cell in the north are more prominent inshore, while the increasing trends further South (e.g. off the Central cell) are more conspicuous offshore. For  $SE_{trend}$ , the area impacted by positive trends surpasses that of negative trends for diatoms (Fig. 6B), with the alternating latitudinal pattern still evident, most notably the decline in diatom  $SE_{trend}$  off the Northern Cell compared to a more typical increase in  $SE_{trend}$  off the Kunene and Central cells (Fig. 6A).

For dinoflagellates, flagellates and mixed communities, there is a dominance of positive *Frequency* trends over negative, which display both latitudinal (Fig. 5B) and cross-shore (Fig. 5A) variability. The dominance in positive trends for these PFGs is particularly prominent when looking at spatial extent (Fig. 6B), which reflects the expansion of their regional occupation. Coccolithophores are the only PFG that show an overall decline in *Frequency* (Fig. 5C) and a shrinkage in their *Spatial Extent* (Fig. 6B), which is constrained to offshore waters (Fig. 6A) in the south ( $\sim 24\text{--}27^\circ\text{S}$ ) (Fig. 5B and Fig. 6A). The observed  $F_{trend}$  imply a poleward offshore and equatorward inshore shift in diatoms,

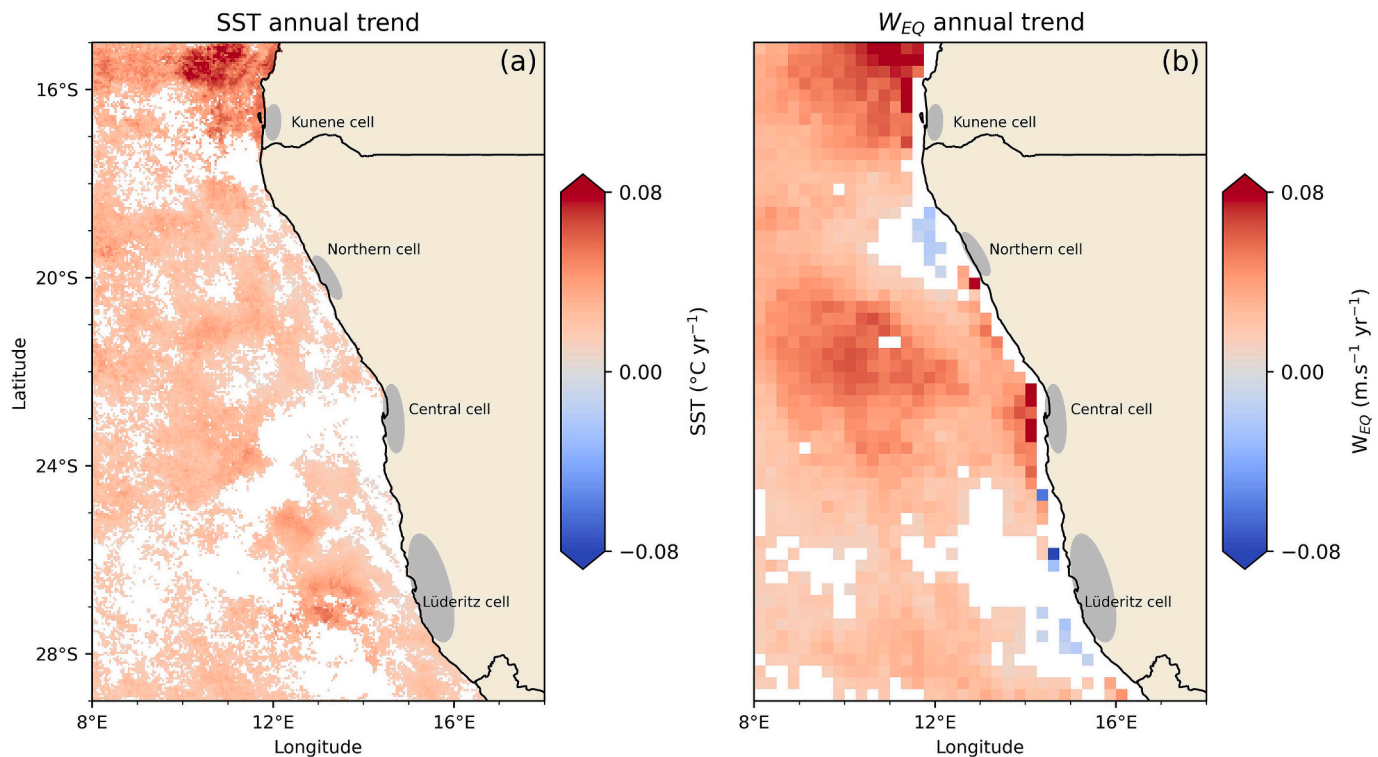


**Fig. 4.** Trends in key climate drivers in the northern Benguela upwelling system.

Annual mean trends in a) sea surface temperatures (SST,  $^{\circ}\text{C yr}^{-1}$ ) and b) equatorward winds ( $W_{EQ}$ ,  $\text{m.s}^{-1} \text{yr}^{-1}$ ) derived from daily satellite observations between 01 January 2003–31 December 2022. The gray shaded areas represent upwelling cells. Only statistically significant ( $P < 0.05$ ) trends are shown.

equatorward shifts in dinoflagellates, flagellates and mixed communities with coccolithophores showing no obvious spatial shifting patterns. Perhaps the most striking result is that diatoms are adjusting at rates double (or more) that of other PFGs, underlining their sensitivity to changing environmental conditions. Such shifts signal possible major restructuring of the plankton community composition and diversity, whose magnitude cannot be assessed from changes in *Frequency* and *Spatial Extent* of dominance alone.

Examining trends in *Frequency* and *Spatial Extent* in a seasonal context (as opposed to annually averaged) unveils discrepancies in where and when community adjustments in PFG dominance may be occurring (Fig. S5, Fig. S6 of the Supplementary Material). For example, a latitudinal band may display both significant positive and negative trends for a particular PFG depending on the season, which partially offset each other when annually averaged. This is the case for  $SE_{trend}$  in diatoms which are positive in Autumn ( $\sim 23$  and  $27^{\circ}\text{S}$ ) but negative  $SE_{trend}$  for the same latitudinal band in Summer. Interrogating the trends through a seasonal lens also highlights instances of multi-decadal PFG succession. For example, in summer and winter there is a co-expansion and increase in  $F_{trend}$  between dinoflagellates, flagellates and mixed communities that coincides with decreasing diatoms. Conversely in Autumn, diatom expansion and an increase in *Frequency* is coincident with decreasing  $F_{trend}$  and  $SE_{trend}$  (or no trends) in other PFGs. The dominance of decreasing  $F_{trend}$  and  $SE_{trend}$  trends for coccolithophores are most prevalent in Spring while increased trends in Summer (Fig. S5, Fig. S6 of the Supplementary Material). Overall, with the remarkable exception observed in coccolithophores, there is a net increase in *Frequency* and *Spatial Extent* of PFGs in the nBUS over the past 2 decades (Figs. 5 and 6).

### 3.4. PFGs adjustments in the context of warming and altered equatorward winds

Evaluating phytoplankton community adjustments in the context of

warming and altered  $W_{EQ}$  reveals strong positive and negative correlations that varied regionally (Fig. S7 and S8 of the Supplementary Material). It is worth noting that these analyses do not include additional physicochemical variables that may influence PFGs (e.g. river/land inputs, interactions with other biota and human-induced dynamics). In addition, different environmental variables may be acting antagonistically, additively or otherwise in driving PFG trends, making it challenging to identify the dominant driver of the observed multi-decadal variability. These relationships may also reflect correlation rather than causation, given the complex interactions and linkages between trophic levels in the upper ocean. With this in mind, we use a qualitative approach to examine the long-term driver-response relationships between PFGs against SST and  $W_{EQ}$ , achieved by grouping statistically significant ( $P < 0.05$ ) trends in PFGs ( $F_{trend}$  and  $SE_{trend}$ ) with their respective significant trends (or absence thereof) in SST and  $W_{EQ}$  (Fig. 7). Each grouping is assigned a color, with warm colors denoting an increasing trend in the PFG, while cool colors indicate a decline.

Coccolithophores aside, the largest coincident driver response in  $F_{trend}$  (Fig. 7C) is an increase in PFGs coincident with warming and  $W_{EQ}$ , (most notably for dinoflagellates - orange bar; and less so for diatoms - blue bar). The same combination of drivers (i.e. warming and increased  $W_{EQ}$ ) is similarly coincident with a large decline in  $F_{trend}$  (Fig. 7C), however the spatial distribution patterns differ considerably for each PFG (see Fig. 7A; red dots versus dark green dots). Warming alone also coincides with a large proportion of increasing  $F_{trend}$  (Fig. 7A; magenta dots). For driver response in  $SE_{trend}$ , there is an overwhelming dominance of increasing trends for all PFGs (except coccolithophores) that are notably associated with both warming (magenta dots) and cooling (maroon dots), but with different regional expressions. A combination of warming and increased winds (red dots) also coincides with a large increase in *Spatial Extent* (Fig. 7B, D), however less so for dinoflagellates (orange bar). Coccolithophores are the only PFG that show a dominance in decreasing  $SE_{trend}$  (Fig. 7D; red bar), the majority of which are aligned with an increase in  $W_{EQ}$  together with warming (dark green dots) or an



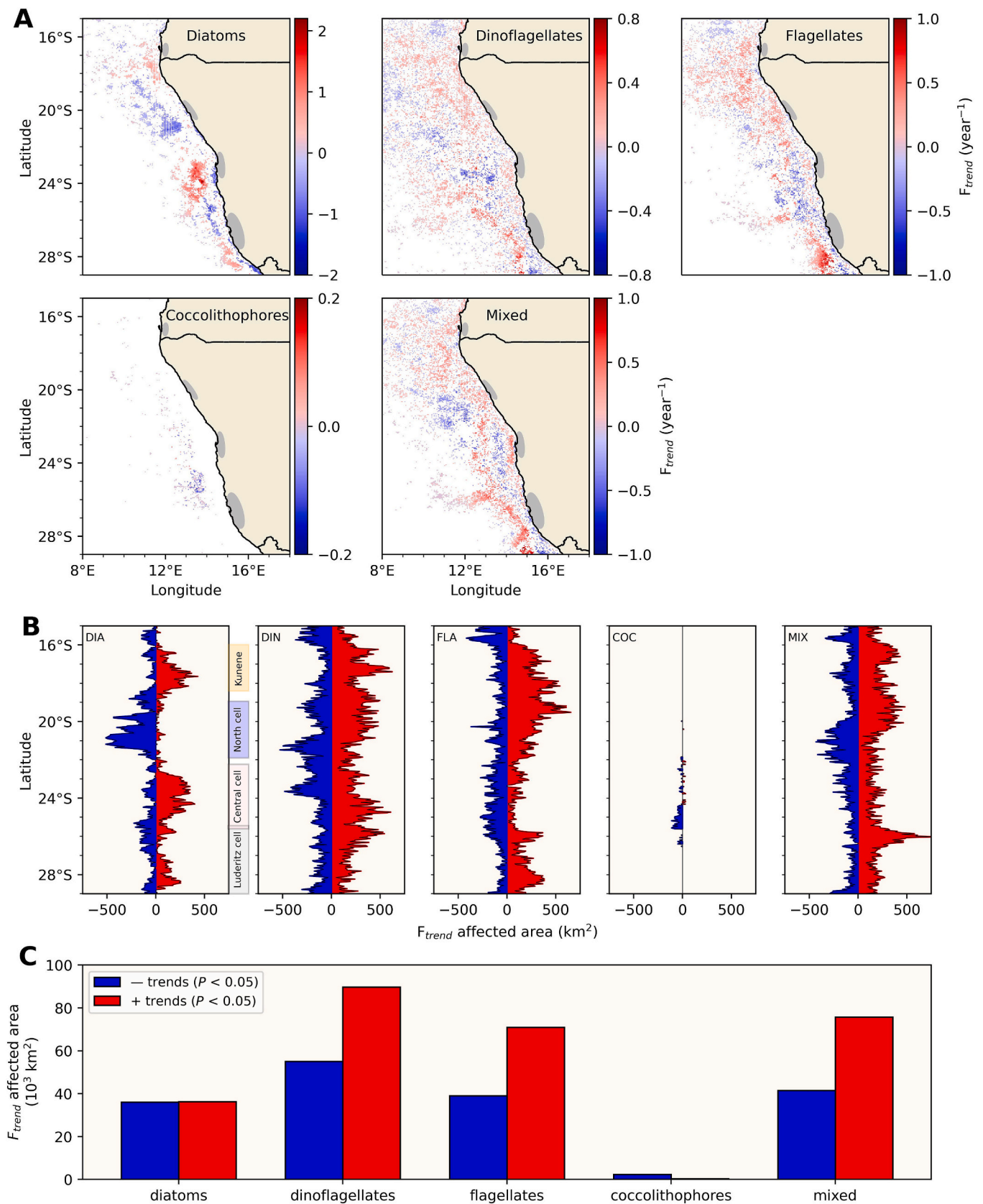


**Fig. 5.** Trends in PFGs Frequency of dominance in the past two decades (2003–2022).

**a.** Spatial patterns of annual trends in Frequency of dominance ( $F_{trend}$ ) of key PFGs. Only statistically significant ( $P < 0.05$ )  $F_{trend}$  are shown. **b.** Latitudinal variation in the area (km<sup>2</sup>) affected by significant negative (blue) and positive (red)  $F_{trend}$  for diatoms (DIA), dinoflagellates (DIN), flagellates (FLA), coccolithophores (COC) and mixed (MIX) communities. Note the varying scales of the annual Frequency trends ( $F_{trend}$ ) colorbars in panel **a** among the PFGs. **c.** delineation of the total area (km<sup>2</sup>) impacted by statistically significant negative (blue) and positive (red) trends.



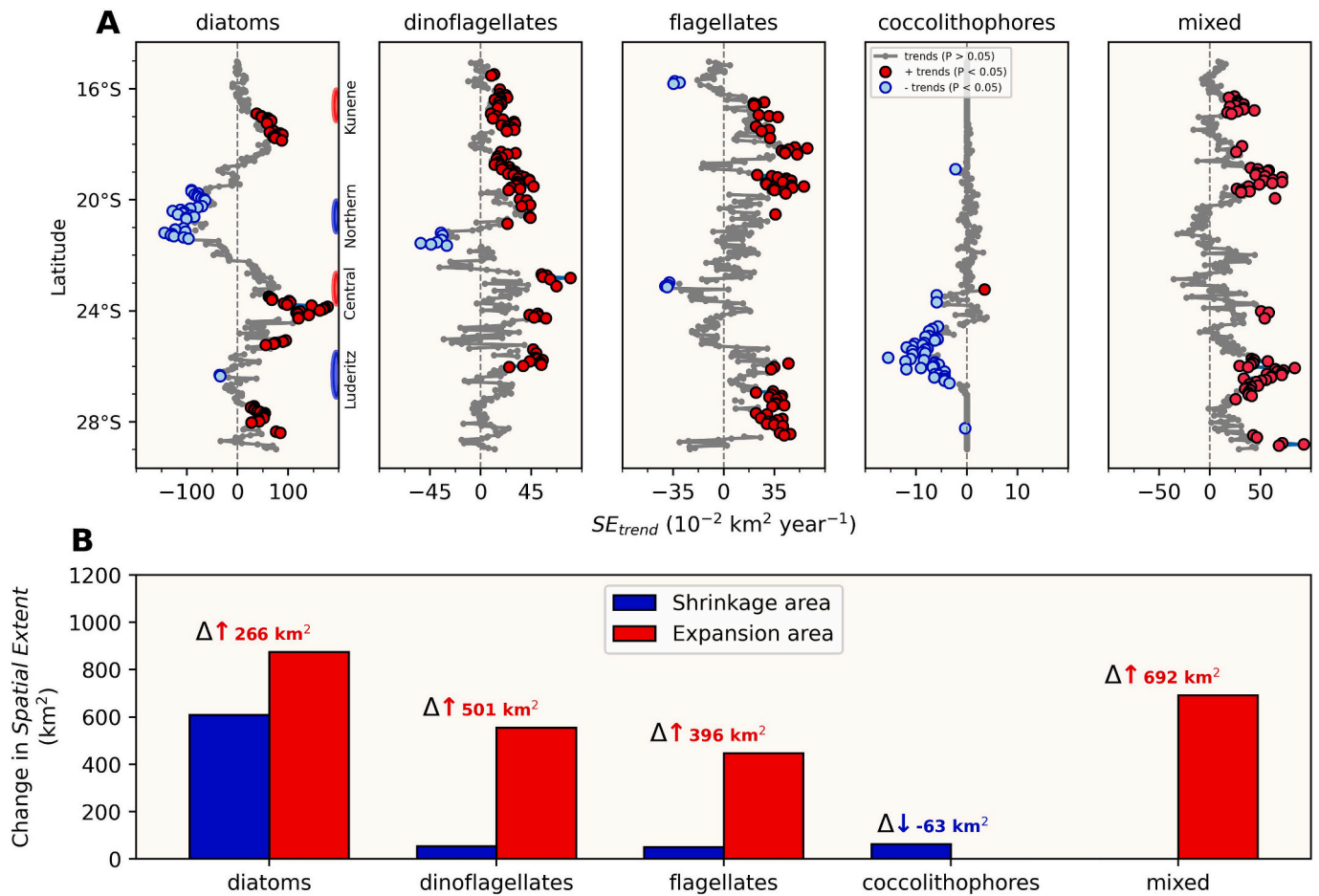


**Fig. 6.** Trends in PFGs Spatial Extent in the past two decades (2003–2022).

**a.** Latitudinal patterns of annual trends in PFG Spatial Extent ( $SE_{trend}$ ). Regions impacted by statistically significant ( $P < 0.05$ ) positive (red dots) and negative (blue dots) indicate expansion and shrinkage in Spatial extent respectively. The gray lines indicate statistically insignificant ( $P > 0.05$ ) trends. **b.** delineation of the total area ( $km^2$ ) impacted by statistically significant negative (blue) and positive (red) trends. Note the varying scales of the annual Spatial extent trends ( $SE_{trend}$ ) in panel a among the PFGs.

increase in  $W_{EQ}$  alone (black dots).

Fig. 8 shows multidecadal trends in Chl-a and co-trends between PFGs and alongshore  $W_{EQ}$  by zooming in on three key subregions associated with upwelling, specifically the Northern (S2 inset box) and Central (S1 and S3 inset boxes) upwelling cells. This focused analysis highlights how localized variability in physical drivers shapes the spatial response of phytoplankton communities. In the Central cell, intensifying alongshore  $W_{EQ}$  coincides with increasing Chl-a and diatoms, declines in coccolithophores and dinoflagellates and no changes in flagellates and mixed communities (Fig. 8a, S1). In contrast, the Northern upwelling cell shows declining alongshore  $W_{EQ}$ , Chl-a, diatoms trends but increasing trends in dinoflagellates, flagellates and coccolithophores (Fig. 8b, S2). Region S3 shows similar  $W_{EQ}$ , Chl-a and PFG trends to S1 but weaker in magnitude (Fig. 8c, S3).

#### 4. Discussion

##### 4.1. Climatological patterns and environmental drivers

Understanding climatological patterns in PFGs is essential for interpreting the timing, composition, and dynamics of primary production, which in turn supports marine food webs and influences biogeochemical cycles (Hubert et al., 2025). Our results reveal well-defined spatial and seasonal structures in PFG distribution across the nBUS, strongly aligned with wind forcing and SST. Diatoms dominated the cooler, nutrient-

enriched coastal regions, particularly during peak upwelling months, while non-diatom groups (flagellates, dinoflagellates, coccolithophores) were more prevalent in warmer, oligotrophic offshore waters (Figs. 2, 3 and S2, S3 of the Supplementary Material). These findings are in agreement with in situ studies conducted in the nBUS, which observed similar spatial zonation and succession patterns in phytoplankton composition in response to upwelling-driven nutrient, SST and water column stability dynamics associated with wind patterns (Hansen et al., 2014; Louw et al., 2016; Mohrholz et al., 2014; Siegel et al., 2007). Whereas previous work has largely relied on in situ datasets at specific locations or short temporal windows, a key advancement of our study is the spatially and temporally explicit, large-scale characterization of PFGs climatology and variability using two decades of daily satellite observations.

##### 4.2. Climate change in the nBUS

The nBUS has been a focus of several studies that documented ongoing warming, expanding oxygen-minimum zones, altered wind patterns and upwelling trends as some of key long-term climate variability (Sweijd and Smit, 2020; Monteiro et al., 2008; Lamont et al., 2018). The observed warming trends (Fig. 1D, 4A and Fig. S4 of the Supplementary Material) are likely to influence the metabolic rates of phytoplankton, with specific functional groups likely outcompeting others under warmer conditions (Soulié et al., 2022). Similarly, trends in

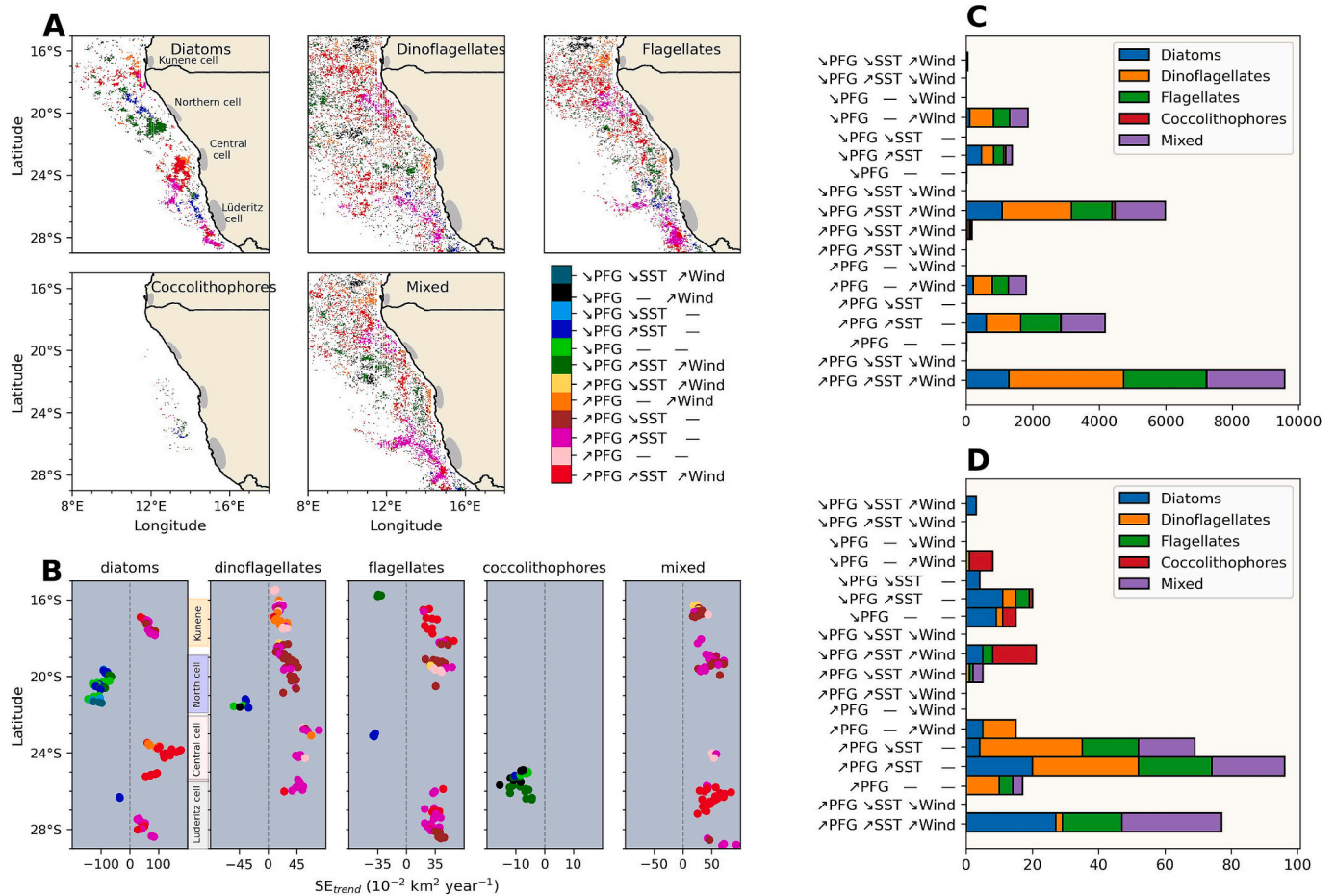


**Fig. 7.** Co-trends between PFGs against equatorward winds and sea surface temperatures.

Spatial distribution of the classification of PFG response to SST and  $W_{EQ}$  between 2003 and 2022 in terms of Frequency (a) and Spatial Extent (b). The co-trends are indicated by different color codes. The dashes indicate statistically insignificant ( $P > 0.05$ ) SST and equatorward wind trends whereas the arrows indicate significant directional trends. Only statistically significant  $F_{trend}$  and  $SE_{trend}$  were included. The counts of co-trends between PFG response ( $F_{trend}$  and  $SE_{trend}$ ) and SST and equatorward winds are shown in c and d, respectively.

nearshore  $W_{EQ}$  bear profound implications for upwelling dynamics, a pivotal process governing nutrient replenishment to the euphotic zone which impacts phytoplankton productivity and community structure (Mohrholz et al., 2014). Specifically, increasing nearshore  $W_{EQ}$  trends relative to the Central and Kunene upwelling cells imply increased nutrient flux (through longer upwelling periods and/or increased upwelling strength) and vice versa for decreasing alongshore  $W_{EQ}$  observed at the Northern and Lüderitz cells, with downstream implications for the success of phytoplankton communities and the marine food web. Previous studies suggest cumulative (overall) decreasing upwelling in the nBUS (Lamont et al., 2018). Our study shows regional variability in alongshore  $W_{EQ}$  trends relative to upwelling cells which suggest that the Lüderitz and Northern upwelling cells are likely the most impacted by decreasing upwelling and may be driving the observed overall reduction in upwelling reported by Lamont et al. (2018).

#### 4.3. PFG adjustments in relation to environmental drivers

In the nBUS, seasonal diatom blooms are typically associated with cooler, nutrient-rich waters following upwelling events, whereas dinoflagellates and flagellates exhibit broader ecological flexibility, thriving in both nutrient-rich upwelled waters and warmer, stratified oligotrophic conditions (Hansen et al., 2014). The observed shifts in diatoms toward areas of accelerating alongshore  $W_{EQ}$  (Kunene and Central cells, Figs. 5, 6, 8 and Fig. S5, S6 of the Supplementary Material) implies a shift to analogous environments of higher nutrient

concentrations, while decreasing trends that align with decelerating alongshore  $W_{EQ}$  (Northern cell) may be attributed to limited nutrient supply from decreased upwelling and/or an intensification of warming induced stratification. This is particularly evident in specific seasons where increasing  $F_{trend}$  and  $SE_{trend}$  in diatoms are coupled with decreasing  $F_{trend}$  and  $SE_{trend}$  in flagellates and dinoflagellates (e.g. Autumn) and vice versa (Summer) (Fig. S5 and S6 of the Supplementary Material), which can be attributed to competitive advantage (Pitcher et al., 1991). These observations imply that competition for resources, particularly with diatoms, may be serving as a mechanism constraining flagellates and dinoflagellates intensification and expansion during periods of increased nutrient flux. Beyond competitive exclusion, physiological stress associated with colder, turbulent, and nutrient-rich upwelled waters due to enhanced upwelling may also limit the proliferation of more motile or light-sensitive groups such as flagellates, dinoflagellates and coccolithophores, which typically perform better under stratified, more stable conditions (Ross and Sharples, 2007). Additionally, shifts in nutrient stoichiometry [e.g. elevated Si:N ratios favoring diatom growth (Allen et al., 2005) or potential imbalances in the Redfield C:N:P ratio] could differentially affect growth and metabolic efficiency across functional groups, as previously shown in the nBUS (Mashifane, 2021). These combined factors likely interact to shape the observed shifts in dominance patterns, particularly across gradients of upwelling cells and offshore distance. These findings align with broader global patterns of phytoplankton community restructuring under climate change, as reported in other major EBUS. For example, in

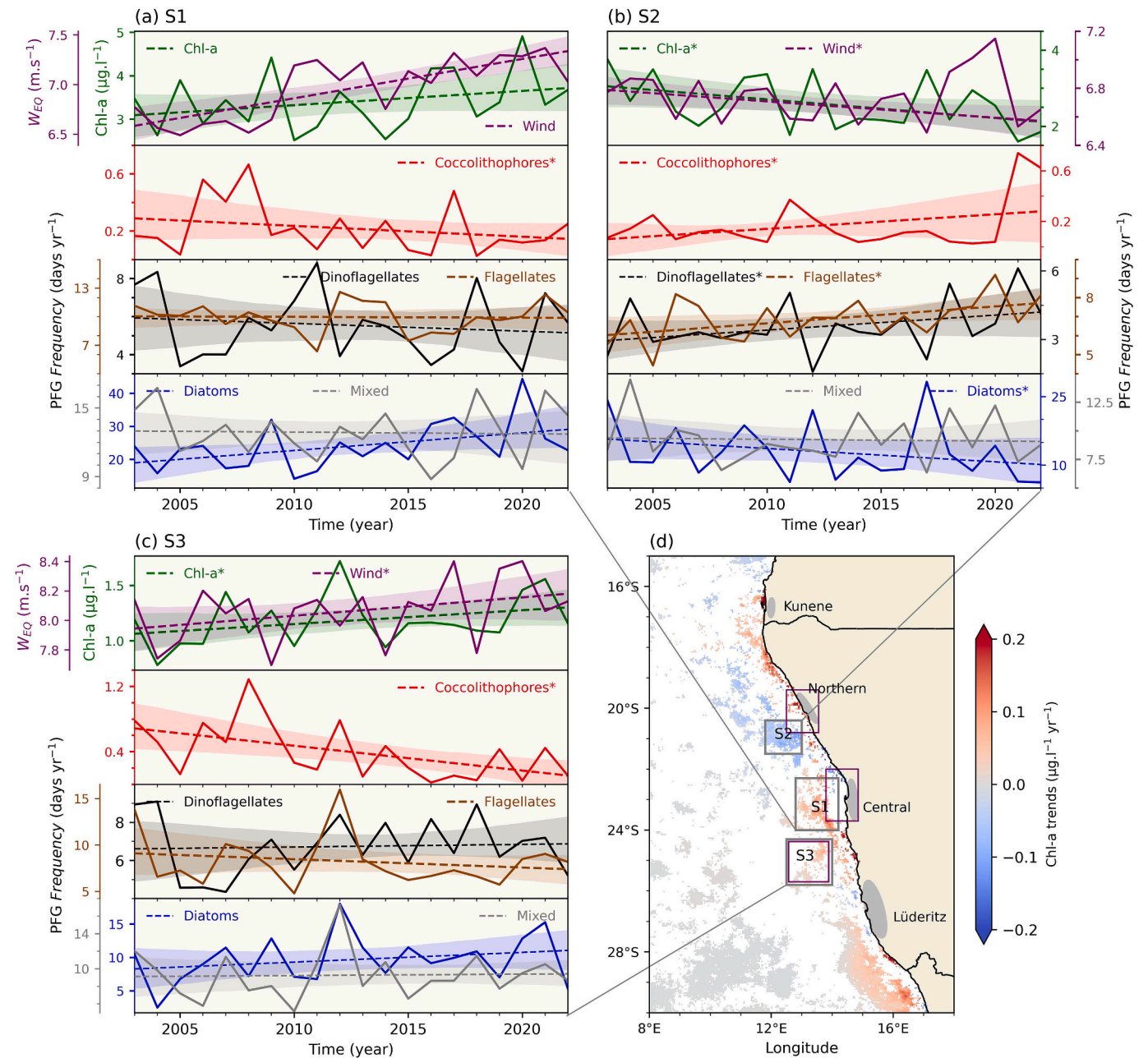


**Fig. 8.** Regional co-trends between PFGs and environmental drivers in the nBUS.

Panels (a)–(c) show multidecadal trends (2003–2022) in diatoms (blue), dinoflagellates (black), flagellates (brown), coccolithophores (red), chlorophyll-a (Chl-a, green) and alongshore equatorward wind ( $W_{EQ}$ , purple) in three regions (S1–S3) associated with major upwelling centers: the Northern and Central upwelling cells. Each subplot highlights the direction and magnitude of trends in PFGs (*Frequency*) alongside corresponding changes in  $W_{EQ}$ . Solid lines show the annual means whereas trends are shown by the dotted straight lines. Equatorward winds ( $W_{EQ}$ ) were computed from the purple boxes relative to boxes S1–S3. Statistically significant ( $P < 0.05$ ) trends are indicated by an asterisk. (d) shows statistically significant spatial Chl-a multidecadal trends.

the California Current System, studies have documented a shift toward flagellates and dinoflagellates during periods of reduced upwelling intensity and warming events (Di Lorenzo and Ohman, 2013). Similarly, the Humboldt Current has shown regional-scale variability in phytoplankton composition in response to long-term changes in wind forcing (Weidberg et al., 2020). These parallels suggest that the PFG adjustments observed in the nBUS are part of a larger trend of ecosystem responses to changing upwelling regimes globally.

On the other hand, coccolithophores thrive in stable and well stratified waters associated with low wind speeds and high solar radiation (Siegel et al., 2007). It is not surprising that their declines are associated with increased offshore  $W_{EQ}$  (notably in Spring; Fig. S6 of the

Supplementary Material), which may be amplifying turbulence and disrupting water column stability.

While there's general warming in the nBUS (Fig. 1D, 6A and Fig. S4 of the Supplementary Material), the observed  $F_{trend}$  and  $SE_{trend}$  likely stem more from adjustments in alongshore  $W_{EQ}$  adjustments relative to upwelling centers, highlighting the dominant role of wind-driven nutrient replenishment, while warming may increase their ability to exploit events of enhanced nutrient availability (Benedetti et al., 2021) and likely drive changes in species diversity (Henson et al., 2021). Overall, with the remarkable exception observed in coccolithophores, there is a net increase in *Frequency* and *Spatial Extent* of PFGs in the nBUS over the past 2 decades (Figs. 5, 6). In this respect, our results (apart



from coccolithophores) support the observations of Dai et al. (2023) who reported bloom intensification and expansion in the past 20 years (2003–2022) for the BUS region as part of a global coastal bloom analysis, albeit not resolving the blooms by PFGs. By focusing on PFGs, our study provides a more nuanced approach to disentangling phytoplankton multidecadal dynamics, which is of particular importance given the varying ecological roles that different functional groups have for ecosystem services. The value of this approach is accentuated by an ability to discern the specific regions and seasons of varying trends in PFGs (Fig. S5 and Fig. S6 of the Supplementary Material). Together, these results enrich our understanding of the underlying mechanisms steering community structure adjustments and highlights the complex associations and competitive interactions among PFGs, potentially serving as a driving force behind the observed spatiotemporal shifts and adjustments in phytoplankton communities.

#### 4.4. Ecological implications of observed adjustments in PFGs

The observed widespread adjustments in phytoplankton community dominance signify possible shifts in energy transfers and biogeochemical cycling within the ecosystem with significant multifaceted ecological implications. These changes can affect primary consumers and cascade to higher trophic levels such as krill, fish, marine mammals and birds, thereby impacting local biodiversity and fisheries yields that sustain local economies in this coastal region. Regions of increased trends in  $F_{trend}$  and  $SE_{trend}$  can potentially benefit commercial fish breeding grounds and food web biodiversity, depending on the functional group that is changing, while the opposite may be true for negative trends. Such adjustments may compel some species to adapt to new diets or result in migration of species that rely on specific phytoplankton to align with their preferred food source. For instance, decreases in energy transfer efficiencies have been associated with a collapse in anchovy larval fish populations in the California current upwelling system and vice versa, stressing the need for sustained quality foods for larval fish survival (Swaethorp et al., 2023). Increasing trends in dinoflagellates are also of concern given their contributing role in the formation of harmful algal blooms, which have the potential to cause devastating economic losses in the aquaculture and fisheries industries through accumulation of biotoxins and anoxia following collapse of high biomass blooms (Ndhlovu et al., 2017). In the current study,  $F_{trend}$  may also signal possible shifts in the phenology of PFGs since the *Frequency* metric relies on counting the number of days of PFG dominance. Increasing  $F_{trend}$  would thus imply PFG dominance that lasts longer and vice versa, which could reflect adjustments in PFGs phenology (e.g. through earlier or delayed bloom initiation, longer or shorter bloom durations). Such shifts in PFG phenologies (e.g. bloom initiation in particular) can potentially desynchronize the timing of food production and important life stages of higher trophic levels, affecting the survival of zooplankton and reproductive success of fish larvae (Cushing, 1990; Platt et al., 2003). A phenology-focused study as a next step is necessary to fully constrain the occurrence and implications of these scenarios in the nBUS.

Our trends analysis reveals a notable seasonal shift in PFGs, with increasing diatoms coinciding with declines in dinoflagellates, flagellates, and coccolithophores in Autumn, and vice versa in Summer (Fig. S5 and S6 of the Supplementary Material). The autumn rise in diatoms may enhance vertical carbon flux and enhance nutritional support to higher trophic levels, particularly zooplankton and pelagic fish that rely on diatom blooms (Moline et al., 2004). In contrast, the summer shifts from diatoms to an expansion of smaller, motile groups like dinoflagellates may lead to reduced carbon sequestration efficiency, as these groups are more prone to recycling in the upper ocean and are less readily grazed by key zooplankton (Moline et al., 2004). These may shift energy flow toward the microbial loop, potentially affecting food web dynamics and fisheries yields at those times of the year.

Given phytoplankton's roles in driving carbon export and air-sea gas

exchanges, adjustments in community composition are likely to affect their role in climate regulation. Diatoms are the most dominant PFG in the nBUS (Figs. 2 and 3) and key role players in the biological carbon pump (BCP) (Allen et al., 2005). Our findings suggest that diatoms are particularly sensitive to climate adjustments, raising concerns for the ecological impact that these changes may elicit. For instance, it is predicted that shifts away from diatom-dominated communities would negatively impact the efficiency of the BCP export and positively feed-back into climate change dynamics (Cerreño et al., 2008). Calcification and the downward flux of calcium carbonate ( $\text{CaCO}_3$ ) by coccolithophores also plays a key role in regulating the carbonate pump (Rost and Riebesell, 2004), which is likely to be negatively impacted by the significant declines in coccolithophores (Figs. 5, 6 and Fig. S5, S6 of the Supplementary Material). Coccolithophores and dinoflagellates also contribute to the global sulfur cycle as prominent dimethylsulfoniopropionate (DMSP) producers (Yoch, 2002). DMSP supports up to 13 % of bacterial carbon and sulfur demand while its cleavage to DMS gas enhances aerosol and cloud formation (Kiene et al., 2000). As such, trends in these key species (declines in coccolithophores but notable increases in dinoflagellates) are likely to alter localized sulfur budgets and DMS emissions with impacts on albedo and climate regulation.

#### 4.5. Limitations of the study

While this study offers valuable insights into the spatial and temporal dynamics of PFGs and their climate-driven responses in the nBUS over the past two decades, several limitations are acknowledged. Firstly, satellite-based detection of phytoplankton is challenged in optically complex waters, particularly in nearshore regions where high concentrations of suspended sediments, chromophoric dissolved organic matter (CDOM), and other particulate matter influence the spectral reflectance. These interferences can obscure phytoplankton signals, potentially resulting in misclassification or underrepresentation of certain groups. The algorithm of Moloto et al. (2023) somewhat accounts for some of these effects through bio-optical parameterization and empirical adjustments, but residual uncertainty remains. Secondly, atmospheric interference from persistent cloud cover, fog, aerosols, and dust, which are common in the region, leads to gaps in satellite observations. These interruptions reduce the number of valid observations, which in turn can underestimate the frequency (daily occurrence) and spatial extent (area coverage) of PFGs. This is particularly problematic for time-series analyses, where consistent temporal coverage is essential for robust trend detection. In this study, we mitigated this issue by applying data screening thresholds and excluding regions or time periods with less than 10 years of data from statistical trend analysis. Thirdly, the current algorithm focuses on dominant and detectable functional groups (diatoms, dinoflagellates, flagellates, coccolithophores, and mixed communities), but does not resolve smaller or less optically distinct groups such as cyanobacteria or green algae. As a result, the ecological contributions of important picophytoplankton taxa, particularly in offshore or oligotrophic regions, are unaccounted for. This constraint reflects the spectral limitations of MODIS-Aqua and the challenges of resolving small-celled taxa from ocean color data. Future studies leveraging upcoming hyperspectral missions (e.g. NASA's PACE mission) may improve classification accuracy and allow inclusion of a more comprehensive range of phytoplankton groups. Lastly, uncertainties in the environmental forcing datasets (e.g. satellite-derived sea surface temperature and wind stress) also influence the interpretation of PFG trends. These drivers are subject to their own limitations in spatial resolution and atmospheric corrections, which may introduce biases in correlating physical conditions with biological responses. Despite these limitations, the study provides robust evidence of climate-associated changes in phytoplankton communities and establishes a valuable baseline for ongoing monitoring and future modeling efforts.



## 5. Conclusions

Our 20-year analysis of PFGs in the nBUS characterizes the regional and seasonal distribution of PFGs and reveals significant multidecadal shifts in response to changes in key physical drivers, notably upwelling-driving  $W_{EQ}$  and SST. Seasonal expansions, contractions, and latitudinal redistributions in dominant PFGs highlight the dynamic and climate-sensitive nature of this ecosystem. These changes have major implications for biogeochemical cycling, food web dynamics, and the sustainability of ecosystem services. Comparisons with previous studies from the southern Benguela and other Atlantic upwelling systems suggest that similar phytoplankton community restructuring is occurring under broader global climate change. Our findings demonstrate the critical value of long-term, high-resolution satellite monitoring for detecting early ecological responses and emphasize the need for continued observation to guide adaptive management. Understanding phytoplankton responses to changing upwelling dynamics provides essential insight for conservation planning, and the development of climate-resilient marine protected areas. These findings can help in identifying climate-sensitive regions and vulnerable seasonal windows where ecosystem shifts are most likely. Targeting these hotspots in marine spatial planning will help develop effective climate-resilient strategies to safeguard the functioning and services of upwelling systems into the future.

## CRedit authorship contribution statement

**Tebatso M. Moloto:** Visualization, Validation, Supervision, Software, Resources, Project administration, Methodology, Investigation, Formal analysis, Data curation, Conceptualization, Writing – review & editing, Writing – original draft. **Sandy J. Thomalla:** Validation, Supervision, Methodology, Investigation, Funding acquisition, Formal analysis, Conceptualization, Writing – review & editing. **Marié E. Smith:** Validation, Supervision, Investigation, Formal analysis, Writing – review & editing. **Thomas G. Bell:** Validation, Supervision, Investigation, Formal analysis, Writing – review & editing. **Stuart J. Piketh:** Supervision, Investigation, Formal analysis, Writing – review & editing.

## Declaration of competing interest

The authors declare no competing interests.

## Acknowledgements

This research was supported as part of the Alliance for Collaboration on Climate and Earth Systems Science (ACCESS)-funded PLankton in a coupled oceAn-aTmOsphere system (PLATO) project by the National Research Foundation [NRF, South Africa, Grant No. 114691] and the Council for Scientific and Industrial Research (CSIR, South Africa) through its Southern Ocean Carbon-Climate Observatory (SOCCO) programme funded by the Department of Science and Innovation (DSI, South Africa) and the parliamentary grant [Grant No. SNA2011112600001]. Additional funding support was provided by Schmidt Sciences LLC under the project "Oxygen and Biogeochemical Dynamics along the West African Margin (WAM): Processes and Consequences". The authors acknowledge the DSI (Department of Science and Innovation)-supported Center for High Performance Computing (CHPC, Rosebank, Cape Town, South Africa) for providing computational resources to this research project. The authors thank Thomas Ryan-Keogh (ORCID: 0000-0001-5144-171X) for providing the python code for spatial trends analysis, Sarah Nicholson (ORCID: 0000-0002-1226-1828) for assistance with wind data processing as well as Sibiso Eric Mbele and Nicolette Chang (ORCID: 0000-0001-7144-7529) for providing technical support with computing on the CHPC cluster.

## Appendix A. Supplementary data

Supplementary data to this article can be found online at <https://doi.org/10.1016/j.scitotenv.2025.180217>.

## Data availability

All the datasets used in this study are publicly available. The MODIS-Aqua reflectance, chlorophyll *a* and sea surface temperature datasets can be found at NASA's Ocean color website at <https://oceancolor.gsfc.nasa.gov/>. The Global Ocean Daily Gridded Reprocessed level 3 (L3) Sea Surface Winds from Scatterometer can be obtained from the E.U. Copernicus Marine Service Information at [doi:10.48670/moi-00183](https://doi.org/10.48670/moi-00183).

## References

- Agenbag, J.J., Shannon, L.V., 1988. A suggested physical explanation for the existence of a biological boundary at 24°30'S in the Benguela system. *S. Afr. J. Mar. Sci.* 6, 119–132. <https://doi.org/10.2989/025776188784480726>.
- Allen, J.T., Brown, L., Sanders, R., Mark Moore, C., Mustard, A., Fielding, S., Lucas, M., Rixen, M., Savidge, G., Henson, S., Mayor, D., 2005. Diatom carbon export enhanced by silicate upwelling in the Northeast Atlantic. *Nature* 437, 728–732. <https://doi.org/10.1038/nature03948>.
- Araújo, C.A.S., Belzile, C., Tremblay, J.-É., Bélanger, S., 2022. Environmental niches and seasonal succession of phytoplankton assemblages in a subarctic coastal bay: applications to remote sensing estimates. *Front. Mar. Sci.* 9, 1001098. <https://doi.org/10.3389/fmars.2022.1001098>.
- Auel, H., Verheye, H.M., 2007. Hypoxia tolerance in the copepod *Calanoides carinatus* and the effect of an intermediate oxygen minimum layer on copepod vertical distribution in the northern Benguela Current upwelling system and the Angola–Benguela Front. *J. Exp. Mar. Biol. Ecol.* 352, 234–243. <https://doi.org/10.1016/j.jembe.2007.07.020>.
- Benedetti, F., Vogt, M., Elizondo, U.H., Righetti, D., Zimmermann, N.E., Gruber, N., 2021. Major restructuring of marine plankton assemblages under global warming. *Nat. Commun.* 12, 5226. <https://doi.org/10.1038/s41467-021-25385-x>.
- Benway, H.M., Lorenzoni, L., White, A.E., Fiedler, B., Levine, N.M., Nicholson, D.P., DeGrandpre, M.D., Sosik, H.M., Church, M.J., O'Brien, T.D., Leinen, M., Weller, R.A., Karl, D.M., Henson, S.A., Letelier, R.M., 2019. Ocean time series observations of changing marine ecosystems: an era of integration, synthesis, and societal applications. *Front. Mar. Sci.* 6, 393. <https://doi.org/10.3389/fmars.2019.00393>.
- Calvin, K., Dasgupta, D., Krinner, G., Mukherji, A., Thorne, P.W., Trisos, C., Romero, J., Aldunce, P., Barrett, K., Blanco, G., Cheung, W.W.L., Connors, S., Denton, F., Diongue-Niang, A., Dodman, D., Garschagen, M., Geden, O., Hayward, B., Jones, C., Jotzo, F., Krug, T., Lasco, R., Lee, Y.-Y., Masson-Delmotte, V., Meinshausen, M., Mintenbeck, K., Mokssit, A., Otto, F.E.L., Pathak, M., Pirani, A., Poloczanska, E., Pörtner, H.-O., Revi, A., Roberts, D.C., Roy, J., Ruane, A.C., Skea, J., Shukla, P.R., Slade, R., Slangen, A., Sokona, Y., Sörensön, A.A., Tignor, M., Van Vuuren, D., Wei, Y.-M., Winkler, H., Zhai, P., Zommers, Z., Hourcade, J.-C., Johnson, F.X., Pachauri, S., Simpson, N.P., Singh, C., Thomas, A., Totin, E., Arias, P., Bustamante, M., Elgizouli, I., Flato, G., Howden, M., Méndez-Vallejo, C., Pereira, J. J., Pichs-Madruga, R., Rose, S.K., Saheb, Y., Sánchez Rodríguez, R., Ürgé-Vorsatz, D., Xiao, C., Yassaa, N., Alegria, A., Armour, K., Bednar-Friedl, B., Blok, K., Cissé, G., Dentener, F., Eriksen, S., Fischer, E., Garner, G., Guivarch, C., Haasnoot, M., Hansen, G., Hauser, M., Hawkins, E., Hermans, T., Kopp, R., Leprince-Ringuet, N., Lewis, J., Ley, D., Ludden, C., Niamir, L., Nicholls, Z., Some, S., Szopa, S., Trewin, B., Van Der Wijst, K.-I., Winter, G., Witting, M., Birt, A., Ha, M., Romero, J., Kim, J., Haïtes, E.F., Jung, Y., Stavins, R., Birt, A., Ha, M., Orendain, D.J.A., Ignon, L., Park, S., Park, Y., Reisinger, A., Cammaramo, D., Fischlin, A., Fuglestedt, J.S., Hansen, G., Ludden, C., Masson-Delmotte, V., Matthews, J.B.R., Mintenbeck, K., Pirani, A., Poloczanska, E., Leprince-Ringuet, N., Péan, C., 2023. IPCC, 2023: Climate Change 2023: Synthesis Report. Contribution of Working Groups I, II and III to the Sixth Assessment Report of the Intergovernmental Panel on Climate Change [Core Writing Team, H. Lee and J. Romero (eds.)]. IPCC, Geneva, Switzerland. Intergovernmental Panel on Climate Change (IPCC). <https://doi.org/10.59327/IPCC/AR6-9789291691647>.
- Carr, M.-E., 2001. Estimation of potential productivity in eastern boundary currents using remote sensing. *Deep Sea Res. Part II Top. Stud. Oceanogr.* 49, 59–80. [https://doi.org/10.1016/S0967-0645\(01\)00094-7](https://doi.org/10.1016/S0967-0645(01)00094-7).
- Carr, M.-E., Kearns, E.J., 2003. Production regimes in four eastern boundary current systems. *Deep Sea Res. Part II Top. Stud. Oceanogr.* 50, 3199–3221. <https://doi.org/10.1016/j.dsr2.2003.07.015>.
- Cermeño, P., Dutkiewicz, S., Harris, R.P., Follows, M., Schofield, O., Falkowski, P.G., 2008. The role of nutrient depth in regulating the ocean carbon cycle. *Proc. Natl. Acad. Sci.* 105, 20344–20349. <https://doi.org/10.1073/pnas.0811302106>.
- Charlson, R.J., Lovelock, J.E., Andreae, M.O., Warren, S.G., 1987. Oceanic phytoplankton, atmospheric Sulphur, cloud albedo and climate. *Nature* 326, 655–661. <https://doi.org/10.1038/326655a0>.
- Cury, P., Shannon, L., 2004. Regime shifts in upwelling ecosystems: observed changes and possible mechanisms in the northern and southern Benguela. *Prog. Oceanogr.* 60, 223–243. <https://doi.org/10.1016/j.pcean.2004.02.007>.

- Cushing, D.H., 1990. Plankton production and year-class strength in fish populations: an update of the match/mismatch hypothesis. In: *Advances in marine biology*. Elsevier, pp. 249–293. [https://doi.org/10.1016/S0065-2881\(08\)60202-3](https://doi.org/10.1016/S0065-2881(08)60202-3).
- Dai, Y., Yang, S., Zhao, D., Hu, C., Xu, W., Anderson, D.M., Li, Y., Song, X.-P., Boyce, D. G., Gibson, L., Zheng, C., Feng, L., 2023. Coastal phytoplankton blooms expand and intensify in the 21st century. *Nature* 615, 280–284. <https://doi.org/10.1038/s41586-023-05760-y>.
- Demarcq, H., 2009. Trends in primary production, sea surface temperature and wind in upwelling systems (1998–2007). *Prog. Oceanogr.* 83, 376–385. <https://doi.org/10.1016/j.pcean.2009.07.022>.
- Di Lorenzo, E., Ohman, M.D., 2013. A double-integration hypothesis to explain ocean ecosystem response to climate forcing. *Proc. Natl. Acad. Sci.* 110, 2496–2499. <https://doi.org/10.1073/pnas.1218022110>.
- Ekau, W., Verheye, H., 2005. Influence of oceanographic fronts and low oxygen on the distribution of ichthyoplankton in the Benguela and southern Angola currents. *Afr. J. Mar. Sci.* 27, 629–639. <https://doi.org/10.2989/18142320509504123>.
- European Union-Copernicus Marine Service, 2017. Global Ocean Daily Gridded Reprocessed L3 Sea Surface Winds from Scatterometer. <https://doi.org/10.48670/MOI-00183>.
- Field, C.B., Behrenfeld, M.J., Randerson, J.T., Falkowski, P., 1998. Primary production of the biosphere: integrating terrestrial and oceanic components. *Science* 281, 237–240. <https://doi.org/10.1126/science.281.5374.237>.
- GEBCO Bathymetric Compilation Group 2023, 2023. The GEBCO 2023 Grid - a continuous terrain model of the global oceans and land. <https://doi.org/10.5285/F98B053B-0C8C-6C23-E053-6C86ABCOAF7B>.
- Hansen, A., Ohde, T., Wasmund, N., 2014. Succession of micro- and nanoplankton groups in ageing upwelled waters off Namibia. *J. Mar. Syst.* 140, 130–137. <https://doi.org/10.1016/j.jmarsys.2014.05.003>.
- He, S., Le, C., He, J., Liu, N., 2022. Empirical algorithm for detecting coccolithophore blooms through satellite observation in the Barents Sea. *Remote Sens. Environ.* 270, 112886. <https://doi.org/10.1016/j.rse.2021.112886>.
- Henson, S.A., Cael, B.B., Allen, S.R., Dutkiewicz, S., 2021. Future phytoplankton diversity in a changing climate. *Nat. Commun.* 12, 5372. <https://doi.org/10.1038/s41467-021-25699-w>.
- Hubert, Z., Louchart, A.P., Robache, K., Epinoux, A., Gallot, C., Cornille, V., Crouvoisier, M., Monchy, S., Artigas, L.F., 2025. Decadal changes in phytoplankton functional composition in the eastern English Channel: possible upcoming major effects of climate change. *Ocean Sci.* 21, 679–700. <https://doi.org/10.5194/os-21-679-2025>.
- Kämpf, J., Chapman, P., 2016. Seasonal wind-driven coastal upwelling systems. In: *Upwelling Systems of the World*. Springer International Publishing, Cham, pp. 315–361. [https://doi.org/10.1007/978-3-319-42524-5\\_8](https://doi.org/10.1007/978-3-319-42524-5_8).
- Kiene, R.P., Linn, L.J., Bruton, J.A., 2000. New and important roles for DMSP in marine microbial communities. *J. Sea Res.* 43, 209–224. [https://doi.org/10.1016/S1385-1101\(00\)00023-X](https://doi.org/10.1016/S1385-1101(00)00023-X).
- Lamont, T., García-Reyes, M., Bograd, S.J., Van Der Lingen, C.D., Sydeman, W.J., 2018. Upwelling indices for comparative ecosystem studies: variability in the Benguela upwelling system. *J. Mar. Syst.* 188, 3–16. <https://doi.org/10.1016/j.jmarsys.2017.05.007>.
- Lamont, T., Barlow, R.G., Brewin, R.J.W., 2019. Long-term trends in phytoplankton chlorophyll *a* and size structure in the Benguela upwelling system. *J. Geophys. Res. Oceans* 124, 1170–1195. <https://doi.org/10.1029/2018JC014334>.
- Louw, D.C., Van Der Plas, A.K., Mohrholz, V., Wasmund, N., Junker, T., Eggert, A., 2016. Seasonal and interannual phytoplankton dynamics and forcing mechanisms in the northern Benguela upwelling system. *J. Mar. Syst.* 157, 124–134. <https://doi.org/10.1016/j.jmarsys.2016.01.009>.
- Mashifane, T.B., 2021. Denitrification and anammox shift nutrient stoichiometry and the phytoplankton community structure in the Benguela upwelling system. *J. Geophys. Res. Oceans* 126, e2021JC017816. <https://doi.org/10.1029/2021JC017816>.
- Mohrholz, V., Eggert, A., Junker, T., Nausch, G., Ohde, T., Schmidt, M., 2014. Cross shelf hydrographic and hydrochemical conditions and their short term variability at the northern Benguela during a normal upwelling season. *J. Mar. Syst.* 140, 92–110. <https://doi.org/10.1016/j.jmarsys.2014.04.019>.
- Moline, M.A., Claustre, H., Frazer, T.K., Schofield, O., Vernet, M., 2004. Alteration of the food web along the Antarctic Peninsula in response to a regional warming trend. *Glob. Change Biol.* 10, 1973–1980. <https://doi.org/10.1111/j.1365-2486.2004.00825.x>.
- Moloto, T.M., Thomalla, S.J., Smith, M.E., Martin, B., Louw, D.C., Koppelman, R., 2023. Remote sensing of phytoplankton community composition in the northern Benguela upwelling system. *Front. Mar. Sci.* 10, 1118226. <https://doi.org/10.3389/fmars.2023.1118226>.
- Monteiro, P.M.S., Van Der Plas, A.K., Mélice, J.-L., Florenchie, P., 2008. Interannual hypoxia variability in a coastal upwelling system: ocean-shelf exchange, climate and ecosystem-state implications. *Deep Sea Res. Part Oceanogr. Res. Pap.* 55, 435–450. <https://doi.org/10.1016/j.dsr.2007.12.010>.
- Ndhlovu, A., Dhar, N., Garg, N., Xuma, T., Pitcher, G.C., Sym, S.D., Durand, P.M., 2017. A red tide forming dinoflagellate *Prorocentrum triestinum*: identification, phylogeny and impacts on St Helena bay, South Africa. *Phycologia* 56, 649–665. <https://doi.org/10.2216/16-114.1>.
- Ohde, T., Siegel, H., Reißmann, J., Gerth, M., 2007. Identification and investigation of Sulphur plumes along the Namibian coast using the MERIS sensor. *Cont. Shelf Res.* 27, 744–756. <https://doi.org/10.1016/j.csr.2006.11.016>.
- Pitcher, G.C., Walker, D.R., Mitchell-Innes, B.A., Moloney, C.L., 1991. Short-term variability during an anchor station study in the southern Benguela upwelling system: phytoplankton dynamics. *Prog. Oceanogr.* 28, 39–64. [https://doi.org/10.1016/0079-6611\(91\)90020-M](https://doi.org/10.1016/0079-6611(91)90020-M).
- Platt, T., Fuentes-Yaco, C., Frank, K.T., 2003. Spring algal bloom and larval fish survival. *Nature* 423, 398–399. <https://doi.org/10.1038/423398b>.
- Reynolds, C.S., Huszar, V., Kruk, C., Naselli-Flores, L., Melo, S., 2002. Towards a functional classification of the freshwater phytoplankton. *J. Plankton Res.* 24, 417–428. <https://doi.org/10.1093/plankt/24.5.417>.
- Ross, O., Sharples, J., 2007. Phytoplankton motility and the competition for nutrients in the thermocline. *Mar. Ecol. Prog. Ser.* 347, 21–38. <https://doi.org/10.3354/meps06999>.
- Rost, B., Riebesell, U., 2004. Coccolithophores and the biological pump: Responses to environmental changes, in: Thierstein, H.R., Young, J.R. (Eds.), *Coccolithophores*. Springer Berlin Heidelberg, Berlin, Heidelberg, pp. 99–125. [https://doi.org/10.1007/978-3-662-06278-4\\_5](https://doi.org/10.1007/978-3-662-06278-4_5).
- Siegel, H., Ohde, T., Gerth, M., Lavik, G., Leipe, T., 2007. Identification of coccolithophore blooms in the SE Atlantic Ocean off Namibia by satellites and in-situ methods. *Cont. Shelf Res.* 27, 258–274. <https://doi.org/10.1016/j.csr.2006.10.003>.
- Smith, M.E., Thomalla, S.J., Matlakala, L., 2023. Coccolithophore bloom classification in coastal waters from multi-decade satellite ocean colour data, in: *Optica Sensing Congress 2023 (AIS, FTS, HISE, Sensors, ES)*. Presented at the Hyperspectral/Multispectral Imaging and Sounding of the Environment, Optica Publishing Group, Munich, p. HW4C.5. doi:<https://doi.org/10.1364/HMISE.2023.HW4C.5>.
- Soulié, T., Vidussi, F., Courboulès, J., Mas, S., Mostajir, B., 2022. Metabolic responses of plankton to warming during different productive seasons in coastal Mediterranean waters revealed by in situ mesocosm experiments. *Sci. Rep.* 12, 9001. <https://doi.org/10.1038/s41598-022-12744-x>.
- Swalethorpe, R., Landry, M.R., Semmens, B.X., Ohman, M.D., Aluwihare, L., Chargualaf, D., Thompson, A.R., 2023. Anchovy boom and bust linked to trophic shifts in larval diet. *Nat. Commun.* 14, 7412. <https://doi.org/10.1038/s41467-023-42966-0>.
- Sweijid, N.A., Smit, A.J., 2020. Trends in sea surface temperature and chlorophyll-a in the seven African large marine ecosystems. *Environ. Dev.* 36, 100585. <https://doi.org/10.1016/j.envdev.2020.100585>.
- Thomalla, S.J., Nicholson, S.-A., Ryan-Keogh, T.J., Smith, M.E., 2023. Widespread changes in Southern Ocean phytoplankton blooms linked to climate drivers. *Nat. Clim. Chang.* 13, 975–984. <https://doi.org/10.1038/s41558-023-01768-4>.
- Tweddle, J.F., Gubbins, M., Scott, B.E., 2018. Should phytoplankton be a key consideration for marine management? *Mar. Policy* 97, 1–9. <https://doi.org/10.1016/j.marpol.2018.08.026>.
- Van Oostende, M., Hieronymi, M., Krasemann, H., Baschek, B., 2023. Global Ocean colour trends in biogeochemical provinces. *Front. Mar. Sci.* 10, 1052166. <https://doi.org/10.3389/fmars.2023.1052166>.
- Weidner, N., Ospina-Alvarez, A., Bonicelli, J., Barahona, M., Aiken, C.M., Broitman, B. R., Navarrete, S.A., 2020. Spatial shifts in productivity of the coastal ocean over the past two decades induced by migration of the Pacific anticyclone and Bakun's effect in the Humboldt upwelling ecosystem. *Glob. Planet. Chang.* 193, 103259. <https://doi.org/10.1016/j.gloplacha.2020.103259>.
- Yoch, D.C., 2002. Dimethylsulfoniopropionate: its sources, role in the marine food web, and biological degradation to Dimethylsulfide. *Appl. Environ. Microbiol.* 68, 5804–5815. <https://doi.org/10.1128/AEM.68.12.5804-5815.2002>.